



LEEDS
BECKETT
UNIVERSITY

Citation:

Zadeh, PB and Sheikh Akbari, A and Buggy, T (2012) Wavelet Based Image Compression Techniques. In: Advances in Wavelet Theory and Their Applications in Engineering, Physics and Technology. InTech China, Unit 405, Office Block, Hotel Equatorial Shanghai, pp. 423-448. ISBN 9789535104940 DOI: <https://doi.org/10.5772/36020>

Link to Leeds Beckett Repository record:

<https://eprints.leedsbeckett.ac.uk/id/eprint/8302/>

Document Version:

Book Section (Published Version)

Creative Commons: Attribution 3.0

The aim of the Leeds Beckett Repository is to provide open access to our research, as required by funder policies and permitted by publishers and copyright law.

The Leeds Beckett repository holds a wide range of publications, each of which has been checked for copyright and the relevant embargo period has been applied by the Research Services team.

We operate on a standard take-down policy. If you are the author or publisher of an output and you would like it removed from the repository, please [contact us](#) and we will investigate on a case-by-case basis.

Each thesis in the repository has been cleared where necessary by the author for third party copyright. If you would like a thesis to be removed from the repository or believe there is an issue with copyright, please contact us on openaccess@leedsbeckett.ac.uk and we will investigate on a case-by-case basis.

Wavelet Based Image Compression Techniques

Pooneh Bagheri Zadeh¹, Akbar Sheikh Akbari² and Tom Buggy²

¹*Staffordshire University,*

²*Glasgow Caledonian University
UK*

1. Introduction

With advances in multimedia technologies, demand for transmission and storage of voluminous multimedia data has dramatically increased and, as a consequence, data compression is now essential in reducing the amount of data prior storage or transmission. Compression techniques aim to minimise the number of bits required to represent image data while maintaining an acceptable visual quality. Image compression is achieved by exploiting the spatial and perceptual redundancies present in image data. Image compression techniques are classified into two categories, lossless and lossy. Lossless techniques refer to those that allow recovery of the original input data from its compressed representation without any loss of information, i.e. after decoding, an identical copy of the original data can be restored. Lossy techniques offer higher compression ratios but it is impossible to recover the original data from its compressed data, as some of the input information is lost during the lossy compression. These techniques are designed to minimise the amount of distortion introduced into the image data at certain compression ratios. Compression is usually achieved by transforming the image data into another domain, e.g. frequency or wavelet domains, and then quantizing and losslessly encoding the transformed coefficients (Ghanbari, 1999; Peng & Kieffer, 2004; Wang et al., 2001). In recent years much research has been undertaken to develop efficient image compression techniques. This research has led to the development of two standard image compression techniques called: JPEG and JPEG2000 (JPEG, 1994; JPEG 2000, 2000), and many non-standard image compression algorithms (Said & Pearlman, 1996; Scargall & Dlay, 2000; Shapiro, 1993).

Statistical parameters of image data have been used in a number of image compression techniques (Chang & Chen, 1993; Lu et al., 2000; Lu et al., 2002; Saryazdi and Jafari, 2002). These techniques offer promising visual quality at low bit rates. However, the application of statistical parameters of the transformed data in image compression techniques has been less reported in the literature. Therefore, the statistical parameters of the transformed image data and their application in developing novel compression algorithms are further investigated in this chapter.

The performance of image compression techniques can also be significantly improved by embedding the properties of the Human Visual System (HVS) in their compression algorithms (Bradley, 1999; Nadenau et al., 2003). Due to the space-frequency localization properties of wavelet transforms, wavelet based image codecs are most suitable for embedding the HVS model in their coding algorithm (Bradley, 1999). The HVS model can be embedded either in the quantization stage (Aili et al., 2006; HSontsch & Karam, 2000; Nadenau et al., 2003), or at the bit allocation stage (Antonini et al., 1992; Sheikh Akbari & Soraghan, 2003; Thornton et al., 2002; Voukelatos & Soraghan, 1997) of the wavelet based encoders. In this chapter, HVS coefficients for wavelet high frequency subbands are calculated and their application in improving the coding performance of the statistical encoder is investigated.

2. Fundamental of compression

The main goal of all image compression techniques is to minimize the number of bits required to represent a digital image, while preserving an acceptable level of image quality. Image data are amendable to compression due to the spatial redundancies they exhibit and also because they contain information that, from a perceptual point of view, can be considered irrelevant. Many standard and non-standard image compression techniques have been developed to compress digital images. These techniques exploit some or all of these image properties to improve the quality of the decoded images at higher compression ratios. Some of these image coding schemes are tabulated in Table 1.

Image compression techniques can be classified into two main groups, named: lossless and lossy compression techniques. In lossless compression process, the original data and the reconstructed data must be identical for each and every data sample. Lossless compression is demanded in different applications such as: medical imagery, i.e. cardiology, to avoid the loss of data and errors introduced into the imagery. Also, it is applied to the case that is not possible to determine the acceptable loss of data.

In most image processing applications, there is no need for the reconstructed data to be identical in value with its original. Therefore, some amount of loss is permitted in the reconstructed data. This kind of compression techniques, which results in an imperfect reconstruction, is called lossy compression. By using lossy compression, it is possible to represent the image with some loss using fewer bits in comparison to a lossless compression.

3. Characteristics of the Human Visual System

Research has shown that embedding the Human Visual System (HVS) model into compression algorithms yields significant improvement in the visual quality of the reconstructed images (Aili et al., 2006; Antonini et al., 1992; Bradley, 1999; HSontsch & Karam, 2000; Nadenau et al., 2003; Sheikh Akbari & Soraghan, 2003; Thornton et al., 2002; Voukelatos & Soraghan, 1997). It has been shown in (Bradley, 1999; Nadenau et al., 2003) that the performance of image compression techniques can be significantly improved by exploiting the limitations of the HVS for compression purposes. To achieve this aim, the HVS-model can be embedded in the compression algorithm to optimise the perceived visual quality.

Standard image coding techniques		Non standard image coding techniques
DCT-base	Wavelet-base	Differential Pulse code Modulation (DPCM) Vector Quantization (VQ) Zero-Tree Coding Fractal Neural Networks Trellis Coding
JPEG (1980)	JPEG2000 (2000)	

Table 1. Standard and non-standard image compression techniques.

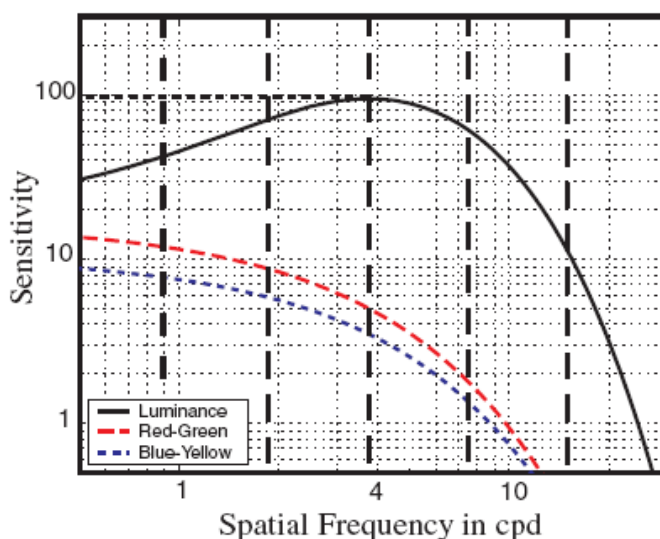


Fig. 1. The CSF curves for the luminance and chrominance channels of the HVS (Nadenau et al., 2003).

Due to the complexity of the human visual processing system, assessments of the performance of HVS-models are based on psychophysical observations. Physiologists have performed many psycho-visual experiments with the goal of understanding how the HVS works. One of the limitations of the HVS, which was found experimentally, is the lower sensitivity of the HVS for patterns with high spatial-frequencies. Exploiting this property of the HVS model, and embedding it into compression algorithms, can significantly improve the visual quality of compressed images. Natural images are composed of small details and

shaped regions. Therefore, it is necessary to describe the contrast sensitivity as a function of spatial frequency. This phenomenon has been known as the Contrast Sensitivity Function (CSF) (Nadenau et al, 2003; Tan et al, 2004). Figure 1 shows the CSF curves for the luminance and chrominance channels of the HVS. From Figure 1, it can be seen that the HVS is more sensitive to the luminance component than the chrominance components. The sensitivity of the HVS in terms of luminance is greatest around the mid-frequencies, in the region of 4 cycles per optical degree (cpd). It rapidly reduces at higher spatial frequencies, and slightly decreases at lower frequencies. The HVS, in terms of chrominance components behaves like a low pass-filter; therefore there is no decrease in its sensitivity at low frequencies.

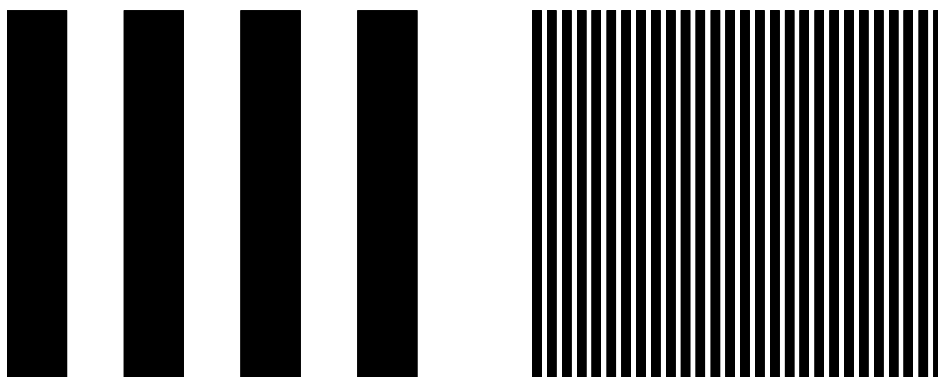


Fig. 2. A low frequency pattern (left) and a high frequency pattern (right), the high frequency pattern appear less intense.

To give a sense of the sensitivity of HVS to different frequencies, two black and white patterns are shown in Figure 2, a low frequency pattern on the left and a high frequency pattern on the right. In both patterns, the black and white have the same brightness, but the black and white colours of the right hand pattern appears less intense than the pattern in the left side. This can be explained by the fact that the HVS is less sensitive to high frequency components.

3.1 Human Visual System in compression techniques

Wavelet-based image coding schemes have proven to be ideally suited for embedding complete HVS models, due to the space-frequency localization properties of the wavelet decompositions (Bradley, 1999). The HVS model has been embedded either at the quantization stage (Aili et al., 2006; HSontsch & Karam, 2000; Nadenau et al., 2003), or at the bit allocation stage (Antonini et al., 1992; Sheikh Akbari & Soraghan, 2003; Thornton et al., 2002; Voukelatos & Soraghan, 1997) of the codec, which yields significant improvement in the visual quality of the reconstructed images. Antonini et al. (Antonini et al., 1992) developed a wavelet-based image compression scheme using Vector Quantization (VQ) and the property of the HVS. This algorithm performs a Discrete Wavelet Transform (DWT) on the input image and then the resulting coefficients in different subbands are vector quantized. The bit allocation among different subbands is based on a weighted Mean

Squared Error (MSE) distortion criterion, where the weights are determined based on the property of the HVS introduced in (Campbell & Robson, 1968). (Voukelatos & Soraghan, 1998) introduced another wavelet based image compression technique using VQ and the properties of the HVS. They first calculated the value of the Contrast Sensitivity Function (CSF) for the central spatial frequency of each subband. These values were then used to scale the threshold value for each subband, which were used in vector selection prior to the VQ process. A weighted MSE distortion criterion using perceptual weights is also employed to allocate bits among different subbands. Voukelatos and Soraghan reported significant improvement over existing block-based image compression techniques at very low bitrates. Thornton et al (Thornton et al., 2002) extended the Voukelatos and Soraghan's algorithm (Voukelatos & Soraghan, 1998) to video for very low bitrate transmission. Thornton et al. incorporated the properties of the HVS to code the intra-frames and reported significant improvement in objective visual quality of the decompressed video sequences. Sheikh Akbari and Soraghan (Sheikh Akbari & Soraghan, 2003) developed another wavelet based video compression scheme using the VQ scheme and the properties of the HVS. They calculated the value of the CSF for the central spatial frequency of each subband of the Quarter Common Intermediate (QCIF) image size. These values were then used to scale the threshold value for each subband, which were used in vector selection prior to the VQ process and also in the bit allocation among different subbands.

The JPEG 2000 standard image codec supports two types of visual frequency weighting: Fixed Visual Weighting (FVW) and Visual Progressive Coding or Visual Progressive Weighting (VPW). In FVW, only one set of CSF weights is chosen and applied in accordance with the viewing conditions, and in the VPW, different sets of CSF weights are used at the various stages of the embedded coding. This is because during a progressive transmission stage, the image is viewed at various distances. For example, at low bitrates, the image is viewed from a relatively large distance, while as more bits are received, the quality of the reconstructed image is increased, which implies that the viewer looks at the image from a closer distance (Skodras et al, 2001). Nadenau et al. incorporated the characteristic of the HVS into a wavelet-based image compression algorithm using a noise-shape filtering stage prior to the quantization stage (Nadenau et al., 2003). They filtered the transformed coefficients using a "HVS filter" for each subband. This algorithm improves the compression ratio up to 30% over the JPEG2000 baseline for a number of test images. A new image compression method based on the HVS was proposed by Aili et al. (Aili et al., 2006). In this codec, the input image is first decomposed using a wavelet transform, and then the transformed coefficients in different subbands are weighted by the peak of the contrast sensitivity function (CSF) curve in the wavelet domain. Finally the weighted wavelet coefficients were coded using the Set Partitioning in Hierarchical Tree (SPIHT) algorithm. This technique showed significantly higher visual and almost the same objective quality to that of the conventional SPIHT technique.

3.2 Calculation of perceptual weights

In this section, the perceptual weights that regulate the quantization steps in different image compression techniques are specifically calculated for a Quarter Common Intermediate Format (QCIF) image size. The derivation of the weighting factors is based on the results of subjective experimental data that was presented in (Van Dyck & Rajala, 1994).

3.2.1 Calculation of spatial frequencies

The perceptual coding model is designed for a QCIF image size, thus this corresponds to a physical dimension of 1.8×2.2 inches on the workstation monitor, i.e. videophone display. Therefore, the pixel resolution r , which is measured in pixels per inch, in both the horizontal and vertical dimensions, will be 80 pixels/inch. Let us assume the viewing distance v , which is measured in metres, be 0.30 metres. This distance is a good approximation of the natural viewing distance of a human using a videophone device. The sampling frequency, f_s in pixels per degree, can be then calculated using Equation 1 (Nadenau et al., 2003):

$$f_s = \frac{2 v \tan(0.5^\circ) r}{0.0254} \quad (1)$$

The signal is critically down-sampled at Nyquist rate to 0.5 cycle/pixel. Hence the maximum frequency represented in the signal is:

$$f_{\max} = 0.5 f_s \quad (2)$$

Thus the maximum frequency represented in the QCIF image size with the thirty centimetre distance will be 8.246 cycles/degree. The centre radial frequency for each subband is determined by the Euclidean distance of its centre from the origin where subbands are in a square of length 8.246 and the base-band is in the origin. Figure 3 shows the centre radial frequencies for each sub-band of a three level wavelet decomposition.

3.2.2 Mean detection threshold

The mean detection threshold is the smallest change in a colour that is noticeable by a human observer and is used to calculate the perceptual weighting factors. It is a function of spatial frequency, orientation, luminance and background colour. The initial data presented in (Van Dyck & Rajala, 1994) was measured in the xY colour space, where x and y are the C.I.E. chromaticity coordinates and Y is the luminance. Table 2 gives the set of thresholds for various frequencies and orientations measured along the luminance, Red-Green and Blue-Yellow directions when the luminance value Y_0 is 5 cd / m^2 and background colour is white. The chromaticity coordinates for white are: $(x_0, y_0) = (0.33, 0.35)$. For transition along the Red-Green and Blue-Yellow direction each mean detection threshold gives two chromaticity coordinates corresponding to the maximum and minimum of the sinusoidal variation as shown in equations 3 and 4, respectively.

$$x_i = x_0 \pm \Delta x \cdot t \quad (3)$$

$$y_i = y_0 \pm \Delta y \cdot t \quad (4)$$

where t is the mean detection threshold, Δx and Δy are the step sizes for the changes in the x and y direction. The values used for Δx and Δy for all three directions are given in Table 3.

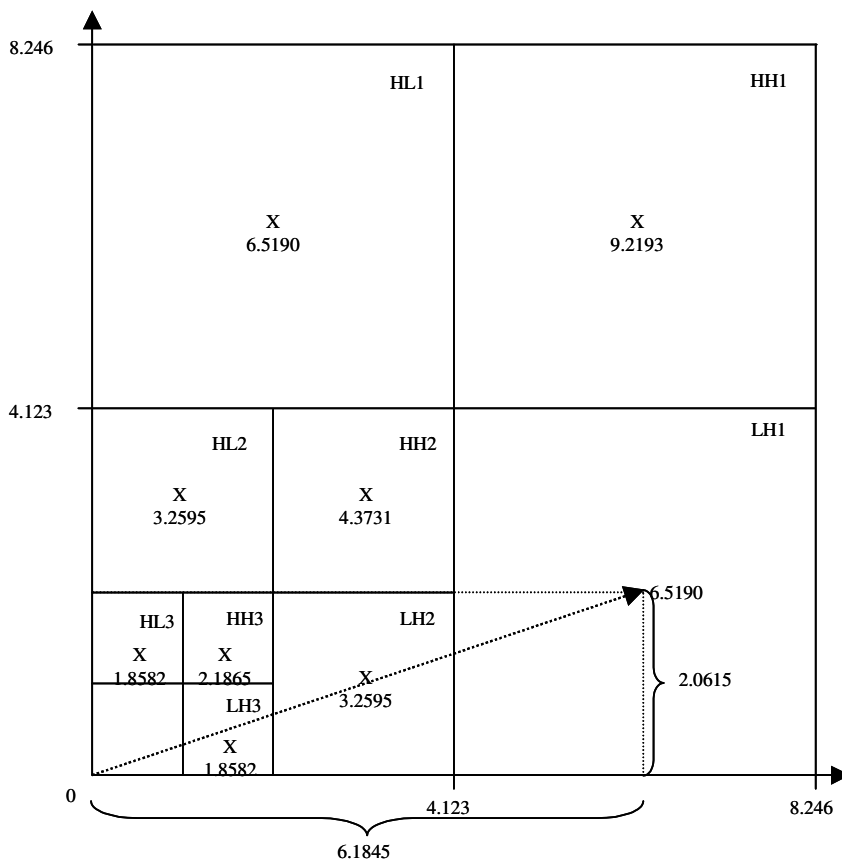


Fig. 3. Subband centre spatial frequencies in cycles/degree.

3.2.3 Perceptual weight factors

The perceptual weight for each subband is the reciprocal of its mean detection threshold. Hence, the mean detection thresholds for the YIQ space need to be calculated before the perceptual weights can be determined. The mean detection thresholds in the xyY space for the centre frequencies of the subbands shown in Figure 3 are first calculated by linearly interpolating the values in Table 2. In wavelet decomposition, the diagonal subbands (HH) do not discriminate between left and right, so an average of the two values is employed. The resulting thresholds in the xyY space for the centre of the high frequency subbands are listed in Table 4. By using equations 3 and 4, two chromaticity coordinates (x_i, y_i, Y_0) , where $i = 1, 2$ for each subband can be calculated. These two chromaticity coordinates are in the xyY space. Therefore they are converted from the xyY space to the C.I.E. XYZ space using the equations in 5: (Ghanbari, 1999).

Spatial Direction	Colour Direction	Spatial frequency cycles/deg				
		1.0	2.0	5.0	10.0	20.0
Horizontal (LH)	Luminance	6.750	6.330	7.250	13.500	65.083
	R-G	4.750	4.750	7.617	17.417	77.417
	B-Y	6.000	6.833	32.667	70.167	150.000
Vertical (HL)	Luminance	6.833	6.250	6.833	22.500	77.800
	R-G	5.583	7.083	9.250	23.000	90.375
	B-Y	6.667	9.417	31.833	65.700	150.000
Left Diagonal (HH)	Luminance	7.667	6.917	11.167	37.083	49.000
	R-G	7.917	7.167	16.083	37.500	100.750
	B-Y	12.417	18.500	45.500	86.500	150.000
Right Diagonal (HH)	Luminance	8.083	7.583	9.167	42.583	85.750
	R-G	7.750	6.333	13.833	35.417	103.500
	B-Y	13.750	19.750	47.750	83.000	114.000

Table 2. Mean detection thresholds in xyY space (Van Dyck 1994).

Direction	ΔY	Δx	Δy
Luminance	0.0124	0.0	0.0
R-G	0.0	0.000655	-0.000357
B-Y	0.0	0.000283	0.000689

Table 3. Step size for changes in each direction (Van Dyck 1994).

SUBBAND	Mean Detection Threshold		
	Luminance	R-G	B-Y
LH1	8.731	9.939	41.554
HL1	10.546	12.508	39.859
HH1	32.436	48.890	75.188
LH2	6.664	5.793	16.236
HL2	6.462	7.871	17.576
HH2	9.556	13.242	40.877
LH3	6.520	4.750	6.454
HL3	6.514	6.402	8.168
HH3	7.431	7.261	20.839

Table 4. Mean detection thresholds in xyY space for subbands.

$$\begin{aligned}
 X_i &= x_i \ Y_0 / y_i \\
 Z_i &= (1 - x_i - y_i) \ Y_0 / y_i \\
 &\text{for } i = 1, 2
 \end{aligned}
 \tag{5}$$

For the luminance direction each mean detection threshold also provides two XYZ values that are calculated using the equations in 6:

$$\begin{aligned}
 X_i &= X_0 \pm \Delta Y \cdot \frac{X_0}{Y_0} \cdot t \\
 Y_i &= Y_0 \pm \Delta Y \cdot t \\
 Z_i &= Z_0 \pm \Delta Y \cdot \frac{Z_0}{Y_0} \cdot t
 \end{aligned}
 \tag{6}$$

where ΔY is given in Table 3, t is the mean detection threshold and $i=1,2$. The vector (X_0, Y_0, Z_0) contains the coordinates of the white point, computed from equation 6. The resulting values are then transformed into the YIQ space. The Red-Green line lies approximately in the I-direction and the Blue-Yellow line lies mostly in the Q direction. The linear transformations in equations 7 and 8 are used to give two points for each direction in the YIQ space.

$$\begin{bmatrix} R \\ G \\ B \end{bmatrix} = \begin{bmatrix} 1.910 & -0.533 & -0.288 \\ -0.985 & 2.000 & -0.028 \\ 0.058 & -0.118 & 0.896 \end{bmatrix} \cdot \begin{bmatrix} X \\ Y \\ Z \end{bmatrix}
 \tag{7}$$

$$\begin{bmatrix} Y \\ I \\ Q \end{bmatrix} = \begin{bmatrix} 0.299 & 0.587 & 0.114 \\ 0.596 & -0.274 & -0.322 \\ 0.211 & -0.523 & 0.312 \end{bmatrix} \cdot \begin{bmatrix} R \\ G \\ B \end{bmatrix}
 \tag{8}$$

The YIQ mean detection threshold for each direction is the inverse Euclidean distance between these two points. The computed weighting factors for each subband of QCIF video, based on the properties of the HVS, are shown in Table 5. These values represent the perceptual weights that can be used to regulate the quantization step-size in the pixel quantization of the high frequency subbands' coefficients of the Multiresolution based image/video codecs.

4. Statistical parameters in image compression

Statistical parameters of the image data have been used in a number of image compression techniques (Chang & Chen, 1993; Lu et al., 2000; Lu et al., 2002; Saryazdi & Jafari, 2002) and have demonstrated promising improvement in the quality of decompressed images, especially at medium to high compression ratios. A vector quantization based image

compression algorithm was proposed by Chang and Chen (Chang & Chen, 1993). It first generates a number of sub-codebooks from the super-codebook, and then employs the statistical parameters of the upper and left neighbour vectors to decide which codebook is to be used for vector quantization. This coding scheme has been extended by Lu et al. (Lu et al., 2000) who generated two master-codebooks, one for the codewords whose variances are larger than a threshold, and another one for the remainder codewords. Lu et al. exploited the current vector's statistical parameter to decide which of these two master codebooks to use for vector quantization, and then Chang and Chen's algorithm was applied to perform vector quantization. Lu et al. (Lu et al., 2002) successfully developed other gradient-based vector quantization schemes and reported further improvement at low bit rates. In the Lu et al. proposed algorithms, one master codebook is first generated and codewords are then sorted in ascending order of their gradient values. In the first algorithm, Chang and Chen's (Chang and Chen, 1993) technique is used to perform vector quantization, with the difference that gradient parameters instead of statistical parameters are used to decide which codebook is to be used for vector quantization. In the second algorithm, the number of codebooks was increased, which resulted in further bit reduction. Another statistically-based image compression scheme was reported by (Saryazdi and Jafari, 2002). In this algorithm, the input image is divided to a number of blocks. The statistical parameters are then used to classify each block into uniform and non-uniform blocks. The uniform blocks are coded by their minimum values. The non-uniform blocks are coded by their minimum and residual values, where the residual values are vector quantized. They reported promising visual quality at high compression ratios.

SUBBAND	Y-DOMAIN	I-DOMAIN	Q-DOMAIN
LH1	4.3807	2.0482	1.0502
HL1	3.4573	1.6159	1.0992
HH1	1.2372	0.6978	0.6065
LH2	5.9673	3.6449	2.6340
HL2	6.1708	2.7149	2.4728
HH2	4.1934	1.6384	1.1331
LH3	6.1796	4.5685	7.1443
HL3	6.1984	3.3243	5.5495
HH3	5.3931	2.9888	2.2339

Table 5. Perceptual weight factors for the YIQ colour domain.

4.1 Distribution of wavelet transform coefficients

Wavelet transform is one of the most popular transform that has been used in many image-coding schemes. As each statistical distribution function has its own parameters, knowledge

of the statistical behaviour of the wavelet transformed coefficients in each subband of an image, can play an important role in designing an efficient compression algorithm. Study of many non-artificial images has shown that distribution of the wavelet-transformed coefficients in high frequency subbands of natural images follow a Gaussian distribution (Altunbasak & Kamaci, 2004; Kilic & Yilmaz, 2003; Eude et al., 1994; Valade & Nicolas, 2004; Yovanof & Liu, 1996). In the following, the Gaussian distribution and its statistical parameters are first reviewed. Then, a review of the study on the distribution of the wavelet transform-coefficients of images is given. A one dimensional Gaussian distribution function $f_g(x)$ is defined as follow:

$$f_g(x) = \frac{1}{\sqrt{2\pi\sigma^2}} e^{-\frac{(x-\mu)^2}{2\sigma^2}} \quad (9)$$

where μ is the mean value of $f_g(x)$ and is calculated using Equation 10:

$$\mu = \int_{-\infty}^{+\infty} x f_g(x) dx \quad (10)$$

and σ is known as the standard deviation, which determines the width the of the distribution. The square of the standard deviation, σ^2 , is called the variance and is determined as follows:

$$\sigma^2 = \int_{-\infty}^{+\infty} x^2 f_g(x) dx \quad (11)$$

where the mean value, μ , and variance, σ^2 , of discrete data, are calculated using Equations 12 and 13, respectively.

$$\mu = \frac{1}{n} \cdot \sum_{i=1}^n x_i \quad (12)$$

$$\sigma^2 = \frac{1}{n} \cdot \sum_{i=1}^n (x_i - \mu)^2 \quad (13)$$

where n is the number of the discrete data, and x_i is the data. Every Gaussian distribution function is defined by two parameters: the mean value, which defines the central location of the distribution, and the variance, which defines the width of the distribution. Four Gaussian distribution functions, with different mean values and variances, are shown in Figure 4.

Study of the distribution of wavelet transform coefficients in each subband has shown that the distribution of the coefficients in the detail subbands of the wavelet-transformed data of natural images is approximately Gaussian (coefficients in the baseband are excluded) [Valade and Nicolas, 2004][Kilic and Yilmaz, 2003]. Distributions of the wavelet coefficients of an image, after applying a three level 2D-wavelet transform, are shown in Figure 5. From Figure 5, it can be seen that except for the lowest frequency coefficients, the distribution of the coefficients in high frequency subbands is approximately Gaussian.

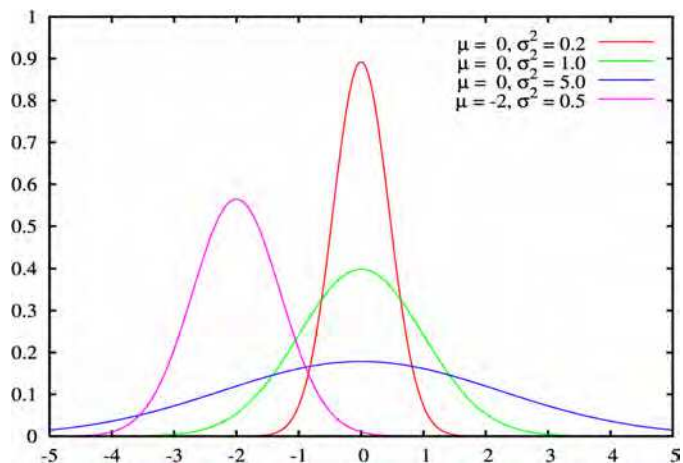


Fig. 4. Gaussian distribution functions (<http://en.wikipedia.org/wiki/Normal-distribution>).

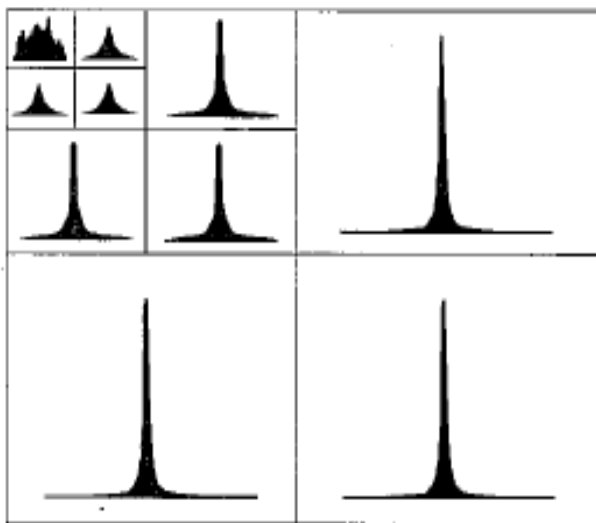


Fig. 5. Histogram of three level wavelet transform of an image (Kilic & Yilmaz, 2003).

In summary, it can be concluded that distribution of the wavelet coefficients in high frequency subbands of natural images can be well approximated by a Gaussian distribution. Therefore, effective use of statistical parameters of the transformed image data (mean values and variances of a Gaussian distribution function) is key in estimation of the transformed data and yielding compression.

4.2 Statistical encoder

In section 4.1 the Gaussian distribution function and its statistical parameters were reviewed. It was shown that every Gaussian distribution function is defined by two parameters: the mean value, which defines the central location of the distribution, and the variance, which defines the width of the distribution. It was also noted that the distribution of the coefficients in each detail subband of the wavelet-transformed data of the natural images is approximately Gaussian has led to the development of a Statistical Encoding (SE) algorithm. The SE algorithm assumes that the coefficients in the 2D input matrix partly follows the Gaussian distribution. Therefore it estimates those parts through a novel hierarchical estimation algorithm, which codes in a lossy manner those parts with their mean values. The SE algorithm applies a threshold value on the variance of the input data to determine if it is possible to estimate them with the mean value of a single Gaussian distribution function or if it needs further dividing into four sub-matrices. This hierarchal algorithm is iterated on the resulting sub-matrices until the distribution of the coefficients in all sub-matrices fulfils the above criteria. Finally, the SE algorithm takes the Gaussian mean values of the resulting sub-matrices as the estimation value for those sub-matrices. The SE algorithm generates a quadtree-like binary map along with the mean values to keep a record of the location of the sub-matrices, which are estimated with their mean values.

A block diagram of the SE algorithm is shown in Figure 6. A two dimensional matrix of size $N \times N$, which for simplification is called U , along with a threshold value, which represents the level of compression, are input to the SE technique. The SE algorithm performs the following process to compress the input matrix U : The SE algorithm first defines two empty vectors called mv (mean value vector) and q (quadtree-like vector). It then calculates the variance (var) and the mean value (m) of the matrix U and compares the resulted variance value with the threshold value. If the variance is less than the threshold value, the matrix is coded by its mean value (m) and one bit binary data equal to 0, which are placed in the mv and q vectors, respectively. If the variance is greater than the threshold, one bit binary data equal to one is placed at the q vector and the size of the matrix is checked. If the size of the matrix is 2×2 , the four coefficients of the matrix are scanned and placed in the mv vector and encoding process is finished by sending the mean value vector mv and the quadtree-like vector q . If the size of the matrix is greater than 2×2 , the matrix U is divided into four equal non-overlapping blocks. These four blocks are then processed from left to right, as shown in Figure 6. For simplify, only the continuation of the coding process of the first block, U_1 , is discussed. This process is repeated exactly on the three other blocks. Processing of the first block U_1 is described as follows: The variance (var_1) and the mean value (m_1) of the sub-matrix U_1 are first calculated and then the resulting variance value is compared with the input threshold value. If it is less than the threshold value, the calculated mean value (m_1) is concatenated to the mean value vector mv and one bit binary data equal to 0 is appended to the quadtree-like vector q . The encoding process of this sub-block is terminated at this stage. Otherwise, the size of the sub-block is checked. If it is 2×2 , one bit binary data equal to 1 is appended to the current quadtree-like vector q and the four coefficients of the sub-block are scanned and concatenated to the mv vector and encoding process is ended for this sub-block. If its size is larger than 2×2 , one bit binary data equal to 1 is concatenated to the

current quadtree-like vector q and the sub-block U_1 is then divided into four equal non-overlapping blocks. These four new sub-blocks are named successor sub-blocks and are processed from left to right in the same way that their four ancestor sub-blocks were encoded. The above process is continued until whole successor blocks are encoded. When the encoding process is finished two vectors mv and q represent the compressed data of the input matrix U .

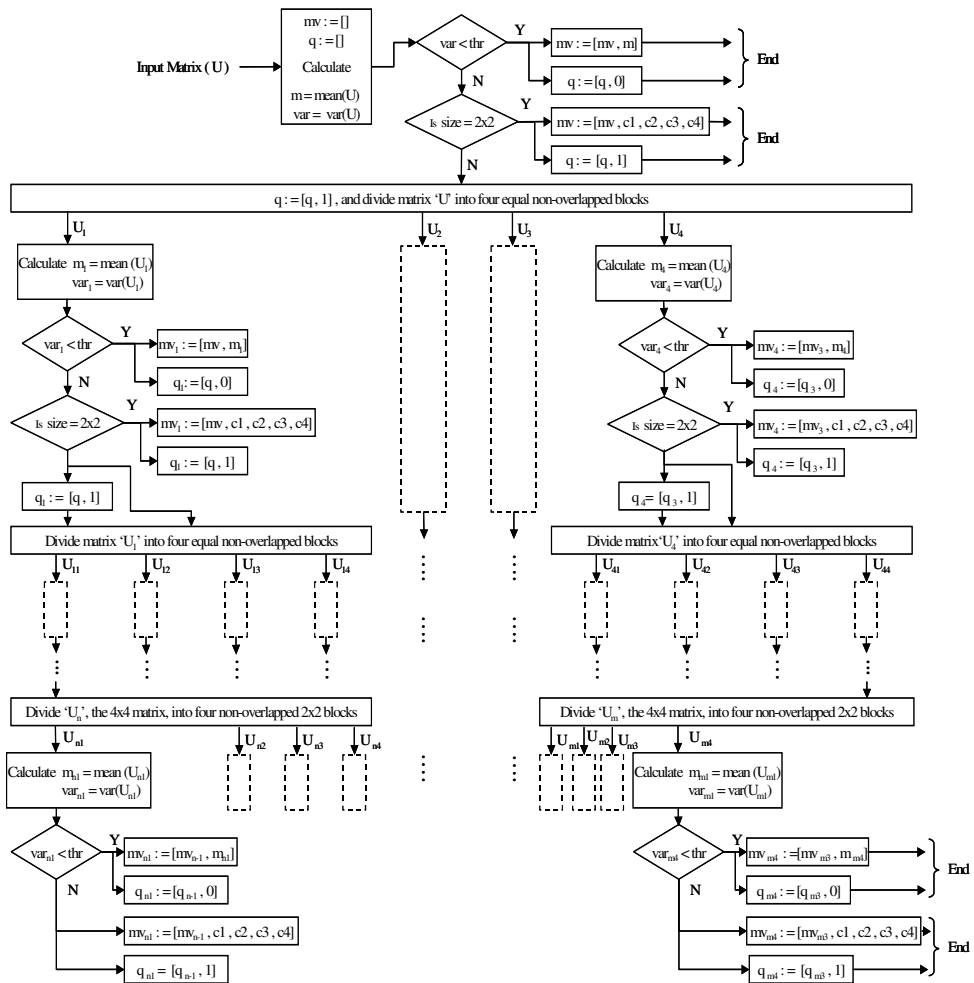


Fig. 6. Block diagram of the Statistical Encoder.

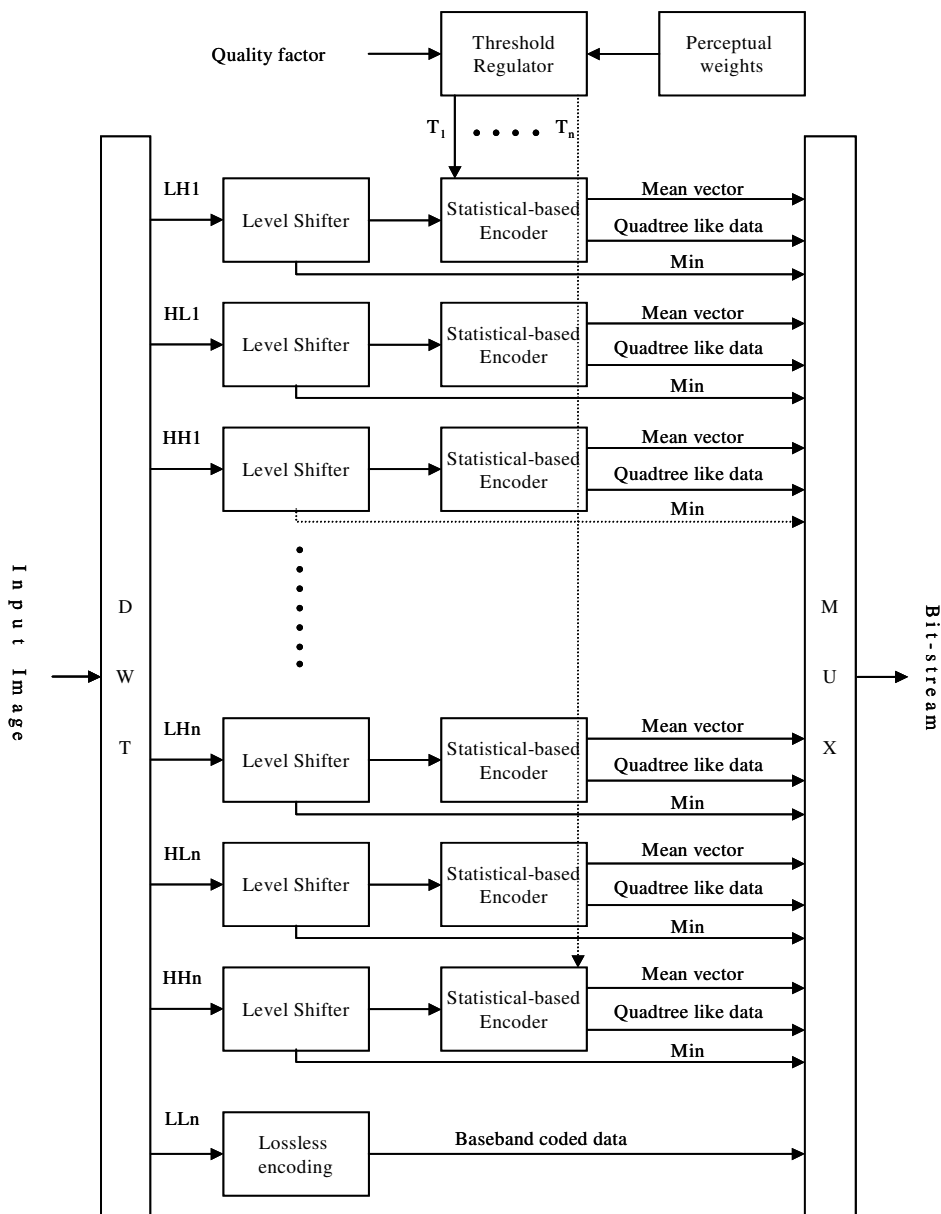


Fig. 7. The multi-resolution and statistical based image encoder.

4.3 Statistical and wavelet based image codec

A block diagram of the Multi-resolution and Statistical Based (MSB) image-coding algorithm is shown in Figure 7. A gray scale image is input to the image encoder. The MSB encoder

then applies a 2D lifting based Discrete Wavelet Transform (DWT) to the input image data and decomposes them into a number of subbands. The DWT concentrates most of the image energy into the baseband. Hence, the baseband is losslessly coded using a Differential Pulse Code Modulation (DPCM) algorithm, which will be explained at the end of this section, to preserve visually important information in the baseband. Coefficients in each detail subband are coded using the procedure that is illustrated in Figure 7 as follows: (i) The coefficients in each detail subband are first level shifted to have a minimum value (Min) of zero; (ii) The resulting level shifted coefficients are then coded using the SE algorithm. The SE algorithm takes the level shifted coefficients of a detail subband and a threshold value, which is specifically designed for that subband, and performs the encoding process (The procedures for generating threshold values for different subbands are explained in Section 4.2.1); (iii) The output of each SE encoder is a mean value vector (mv), which carries the mean values, and a quadtree-like vector (q), which carries the quadtree-like data; (iv) Finally the multiplexor combines all the resulting data together and generates the compressed output bitstream.

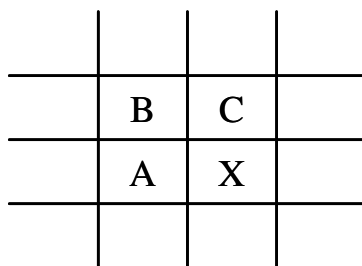


Fig. 8. Three-sample prediction neighbourhoods for DPCM method.

In the DPCM method pixel X with the value of x , is predicted from its three neighbouring pixels, called: A , B and C , with the values of a , b and c respectively, as shown in Figure 8. The prediction value of pixel X , called P_x , is calculated using Equation 14:

$$P_x = b + \frac{a - c}{2} \quad (14)$$

The predicted value of pixel X is then subtracted from the actual value of pixel X to generate an error value, and all the resulting error values are finally losslessly coded.

4.3.1 Threshold generation

In this research work, perceptual weights are employed to regulate the threshold values for different subbands. Hence, the threshold value for each detail subband is generated using a uniform quality factor divided by the perceptual weight of the centre of that subband, where the uniform quality factor can take any positive value. There is a direct relationship between the uniform quality factor and the resulting compression ratios. In Section 3.2 an algorithm for calculating the perceptual weights for detail subbands of a wavelet transformed image data was given. The proposed algorithm is used to calculate the perceptual weights for the centre of each detail subband of an image of size 512×512 and a viewing distance of 40 centimetres, which are shown in Table 6.

DWT Level	Subband	Y-Domain	I-Domain	Q-Domain
ONE	LH	3.0230	1.3251	0.7258
	HL	2.0443	1.0275	0.7681
	HH	0.8713	0.4273	0.4697
TWO	LH	5.4726	2.9355	1.6570
	HL	5.5166	2.3270	1.6560
	HH	2.4531	1.0992	0.8321
THREE	LH	6.1930	4.2479	4.9906
	HL	6.3060	2.9823	4.0070
	HH	4.8143	2.2390	1.6068

Table 6. Perceptual weights for the YIQ colour domain (512×512 image size and a viewing distance of 40 cm).

4.3.2 Results

In order to evaluate the performance of the proposed MSB codec two sets of experiments were performed. In the first sets of experiments the performance of the MSB codec using perceptual weights is compared to that of MSB without using perceptual weights to regulate the threshold values for different subbands, which are presented in Sub-section 4.3.2.1 In the second sets of experiments, the MSB codec using perceptual weights is compared to those of JPEG and JPEG2000 standard image codecs, where the results are illustrated in Sub-section 4.3.2.2.

4.3.2.1 Results for the codec with and without using perceptual weights

The performance of the MSB image codec was investigated on three greyscale test images (with resolution of 8-bits per pixel) and size of 512×512 pixels: 'Lena', 'Elaine', and 'House'. These test images cover all range of spatial frequencies from very low frequency smooth areas, to textures with middle frequencies, and very high frequency sharp edges. In order to evaluate the effect of the perceptual weights on the performance of the proposed codec, 'Lena', 'Elaine', and 'House' test images were compressed using the proposed codec with and without using perceptual weights to regulate the uniform threshold value for different subbands. A three level Daubechies 9/7 wavelet transform was used to decompose the input image into ten subbands for this experiment. The PSNR criterion was used to evaluate the quality of the reconstructed images. The PSNR measurements for the test images at different compression ratios using the MSB codec

with and without perceptual weights are given in Figure 9(a) to 9(c) respectively. From these Figures, it is clear that the MSB codec using perceptual weights gives significantly higher performance to that of the MSB codec without perceptual weights. However, it is well known that the PSNR is an unreliable metric for measuring the visual quality of the decompressed images (Kaia et al., 2005). Hence, to illustrate the true visual quality obtained using the MSB codec with and without perceptual weights, the reconstructed 'Lena', 'Elaine', and 'House' images at compression ratio of 16 using the proposed codec are shown in Figure 10(I) to 10(III), respectively. From these figures, it can be seen that the reconstructed images, when perceptual weights are used in the encoding process, have significantly higher visual quality with less blurred edges and better surface details. From Figure 10(I) and 10(II), which show decoded 'Lena' and 'Elaine' test images, it is obvious that the images using the MSB codec using perceptual weights have a noticeably higher quality to those decoded using the MSB codec without employing perceptual weights. It can also be seen that the decoded test images using the MSB codec with perceptual weights have clearer facial details with less blurring in the faces. From Figure 10(III) it is clear that the reconstructed 'House' test image using MSB with HVS have significantly higher visual quality with lower blurred edges and clearer surface details.

4.3.2.2 Results of the MSB, JPEG and JPEG2000 codecs

In this section, the performance of the MSB codec with perceptual weights is compared to JPEG and JPEG2000 (JPEG2000, 2005) standard image coding techniques. The MSB, JPEG and JPEG2000 were used to compress 'Lena', 'Elaine', and 'House' test images at different compression ratios. The PSNR measurements for the encoded images using the MSB, JPEG, and JPEG2000 image codecs at different compression ratios are shown in Figures 11(a) to 11(c), respectively. From these figures it can be seen that the MSB codec gives superior performance to JPEG and JPEG2000 at low compression ratios. From Figure 11(a) and 11(b), it can be observed that the proposed codec offers higher PSNR in coding 'Lena' and 'Elaine' test images to those of JPEG and JPEG2000 at compression ratios lower than 5. From Figure 11(c), it is clear that the MSB codec outperforms JPEG and JPEG2000 in coding 'House' test images at compression ratios of up to 4. However, it is well known that the PSNR often does not reflect the visual quality of the decoded images, thus a perceptual quality evaluation seems to be necessary. To demonstrate the visual quality achieved using the MSB, JPEG and JPEG2000 coding techniques at different compression ratios, the decoded 'Lena' and 'Elaine' test images at compression ratios 5 and 40 using these techniques are shown in Figures 12 and 13, respectively.

From Figures 12(a), it can be seen that the visual quality of the decoded Lena test image at a compression ratio of 5 using MSB codec is high. It is also clear that the quality of the decoded Lena test image using MSB codec is slightly higher than that of JPEG and almost the same as that of JPEG2000. The Elaine test image contains significant high frequency details and is more difficult to code. From Figure 12(b), which illustrates the decoded Elaine test images at compression ratio of 5, the high visual quality of all the decoded images is obvious. From Figures 13(a), which illustrates the decoded Lena test images at a compression ratio of 40, the severe blocking artefact of the decoded image using JPEG is quite obvious, where the MSB decoded image contains some blurring around the mouth

and ringing artefacts around edges in the image. In terms of overall visual quality, the MSB decoded Lena test image has superior visual quality to that of JPEG. It is also clear that the quality of the MSB decoded image is slightly inferior to that of JPEG2000. From Figures 13(b), which illustrates the decoded Elaine test images at a compression ratio of 40, it is obvious that: a) the decoded JPEG image exhibits severe blocking artefacts; b) the MSB decoded image has higher visual quality but suffers from blurring in the background of the image and ringing artefacts in its sharp edges and c) the JPEG2000 decoded image has high visual quality but slight blurring and ringing artefacts can be seen in some regions of the background and sharp edges of the image. It is clear that the JPEG2000 decoded images have slightly higher visual quality than MSB decoded images.

The results presented here demonstrate that the MSB codec outperforms JPEG and JPEG2000 image codecs, subjectively and objectively, at low compression ratios (up to compression ratio of 5). The results also show that at middle-range compression ratios JPEG decoded images somewhat suffer from blocking artefacts, while the visual quality of the MSB decoded images is significantly higher.

The results at high compression ratios (around 40) indicate that a) the JPEG decoded images severely suffer from blocking artefacts, so much so that there is no point in using JPEG to code images at high compression ratios; b) the MSB decoded images have significantly higher visual quality than that of JPEG, while they slightly suffer from patchy blur in regions with soft texture and ringing noise at sharp edges; c) decoded MSB images have significantly lower PSNR in comparison to that of JPEG2000 but their visual quality is slightly inferior to that of JPEG2000.

5. Conclusion

In this Chapter first a novel statistical encoding algorithm was presented. The proposed SE algorithm assumes that the distribution of the coefficients in the input matrix is partly Gaussian and uses a hierarchical encoding algorithm to estimate the coefficients in the input matrix with the Gaussian mean values of multiple distributions; then a multi-resolution and statistical based image-coding scheme was developed. It applies a 2D wavelet transform on the input image data to decompose it into its frequency subbands. The baseband is losslessly coded to preserve the visually important image data. The coefficients in each detail subband were first dc level shifted to have a minimum value of zero and then coded using the SE algorithm. The SE algorithm takes the dc level shifted coefficients of a detail subband and a threshold value, which is generated for that subband. The encoding process is then performed. Perceptual weights were calculated for the centre of each detail subband and used to regulate the threshold value for that subband.

Experimental results showed that the proposed coding scheme provides significantly higher subjective and objective quality when perceptual weights are used to regulate the threshold values. The results also indicated that the proposed codec outperforms JPEG and JPEG2000 coding schemes subjectively and objectively at low compression ratios. Results showed that the proposed coding scheme outperforms JPEG subjectively at higher compression ratios. It offers comparable visual quality to that of JPEG2000 at high compression ratios.

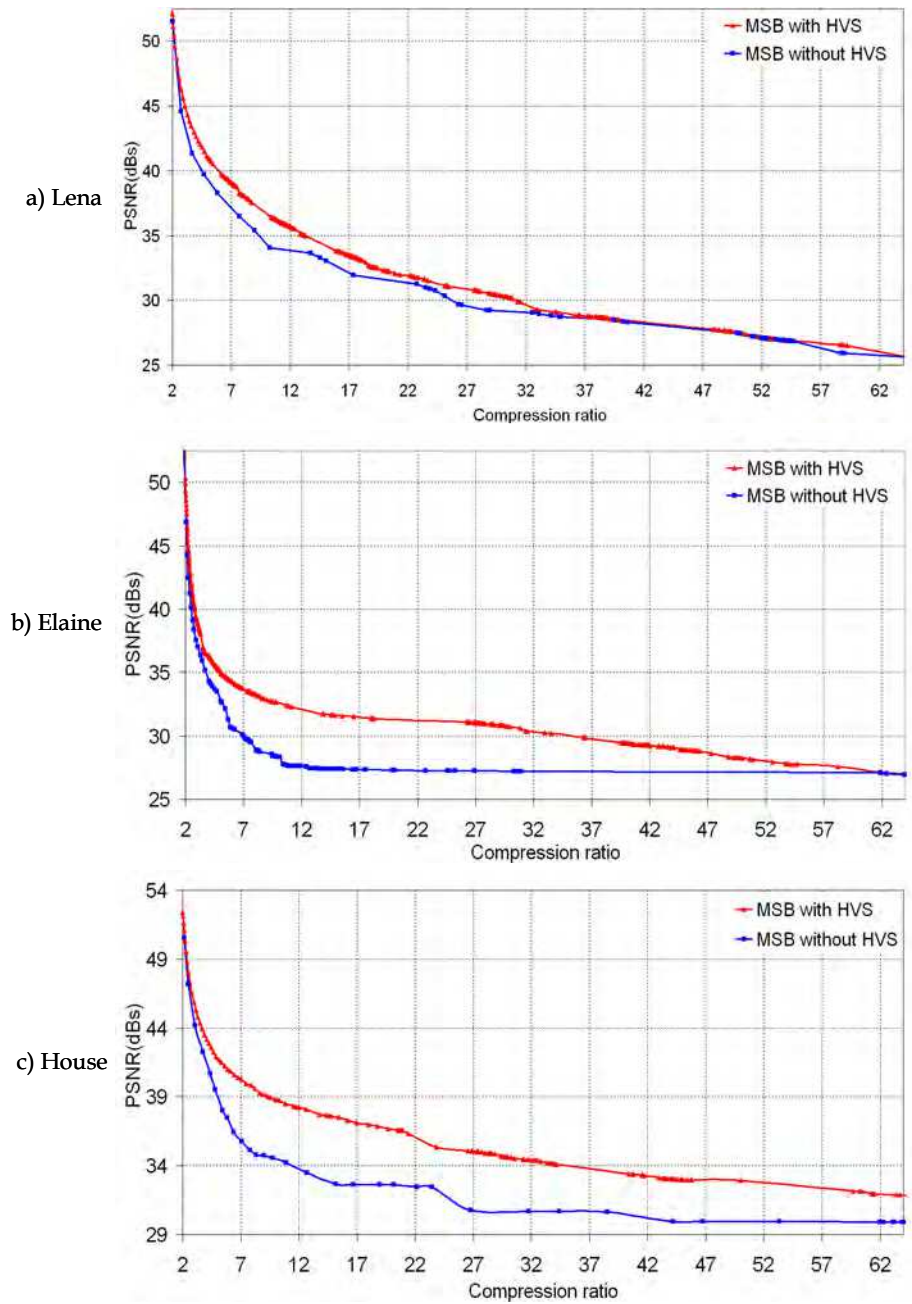


Fig. 9. PSNR measurements for a) 'Lena', b) 'Elaine' and c) 'House' test images at different compression ratios using MSB codec with and without employing perceptual weights.



Fig. 10. Reconstructed I) 'Lena', II) 'Elaine' and II) 'House' test images at compression ratio of 16 using the MSB codec a) with HVS and b) without HVS.

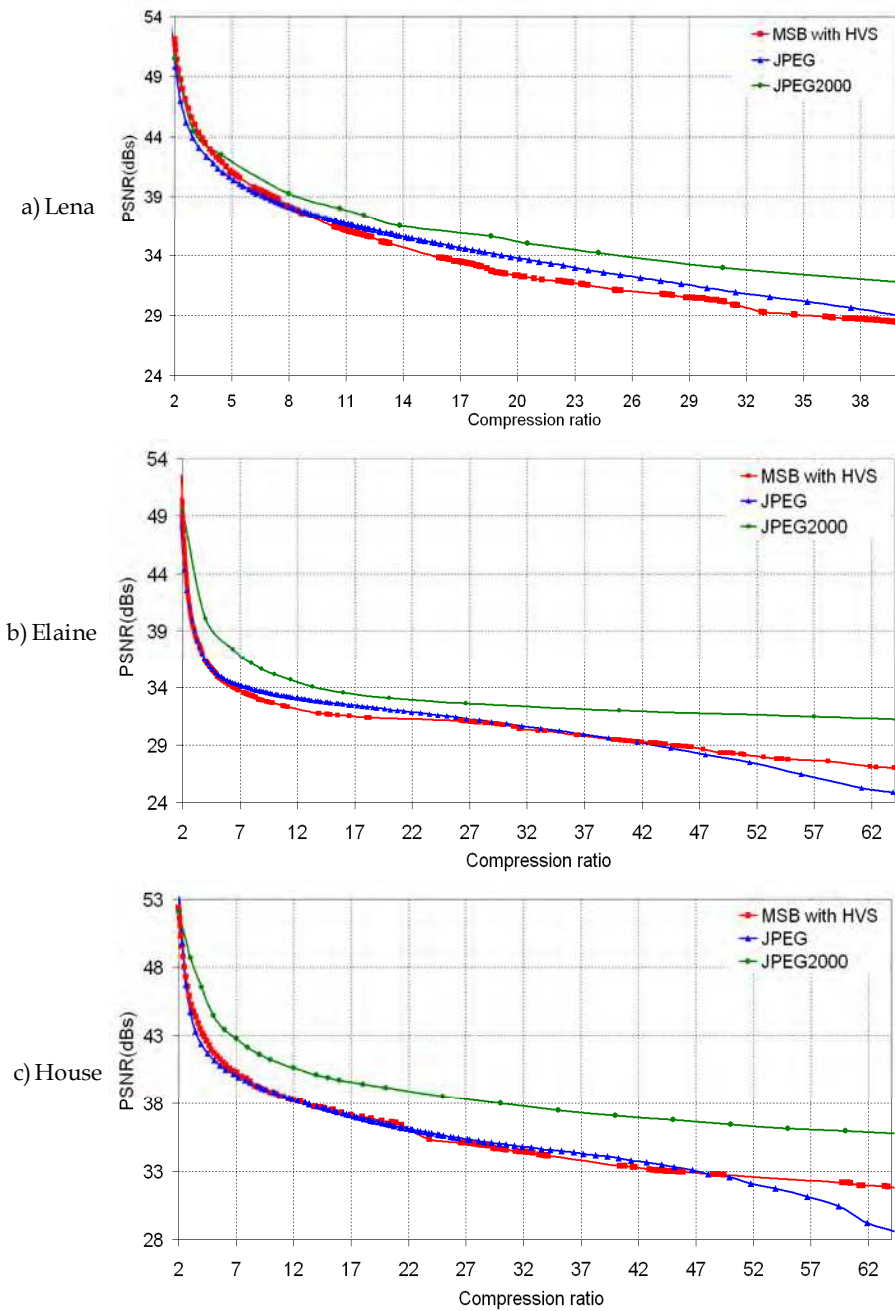


Fig. 11. PSNR measurements for a) 'Lena', b) 'Elaine' and c) 'House' test images at different compression ratios using MSB, JPEG and JPEG2000 codecs.

I) MSB



II) JPEG



III) JPEG 2000



a) Lena

b) Elaine

Fig. 12. Reconstructed a) 'Lena' and b) 'Elaine' test images at compression ratio of 5 using I) MSB codec, II) JPEG and III) JPEG2000.

I) MSB



II) JPEG



III) JPEG 2000



a) Lena

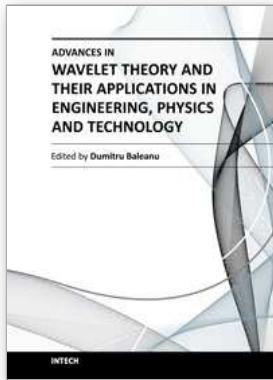
b) Elaine

Fig. 13. Reconstructed a) 'Lena' and b) 'Elaine' test images at compression ratio of 40 using I) MSB codec, II) JPEG and III) JPEG2000.

6. References

- (Aili et al., 2006) W. Aili, Z. Ye and G. Yanfeng, "SAR Image Compression Using HVS Model", International Conference on Radar 2006, pp. 1-4, Oct. 2006.
- (Altunbasak & Kamaci, 2004) Y. Altunbasak and N. Kamaci, "An Analysis Of The DCT Coefficient Distribution with The H.264 Video Coder", *ICASSP2004*, pp.178-180, 2004.
- (Antonini et al., 1992) M. Antonini, M Barlaud, P. Mathieu and I. Daubechies, "Image coding using the wavelet transform," *IEEE Transaction on Image Processing*, Vol. 1, No. 2, pp. 205-220, April 1992.
- (Bradley, 1999) A. P. Bradley, A wavelet visible difference predictor, *IEEE Transaction on Image Processing*, vol.8, no. 5, 1999.
- (Campbell & Robson, 1968) F.W. Campbell and J. G. Robson, "Application of Fourier Analysis to the Visibility of Gratings", *Journal of Physiologic*, vol. 197, pp. 551-566, 1968.
- (Eude et al., 1994) T. Eude, H. Cherifi and R. Grisel, "Statistical distribution of DCT coefficients and their application to an adaptive compression algorithm", *IEEE International Conference TENCON1994*, pp. 427-430, 1994.
- (Ghanbari, 1999) M. Ghanbari, "Video coding an introduction to standard codecs," *Published by: The Institution of Electrical Engineering, London, UK, 1999.*
- (Chang & Chen, 1993) R. F. Chang and W. T. Chen, "Image Coding Using Variable-Rate Side-Match Finite-State Vector Quantization," *IEEE Transaction on Image Processing*, vol. 2, no. 1, January 1993.
- (HSontsch & Karam, 2000) I. Höntsch and L. Karam, "Locally adaptive perceptual image coding," *IEEE Transaction on Image Processing*, vol. 9, no. 9, pp. 1472-1483, September 2000.
- (JPEG, 1994) Information Technology-JPEG-Digital Compression and Coding of Continuous-Cone Still Image-Part 1: Requirement and Guidelines, 1994. ISO/IEC 10918-1 and ITU-T Recommendation T.81.
- (JPEG2000, 2000) JPEG 2000 Part I Final Committee Draft Version 1.0, ISO/IEC JTC1/SC29/WG1 N1646R, Mar. 2000.
- (Kilic & Yilmaz, 2003) I. Kilic and R. Yilmaz, "A Video Compression Technique Using Zerotree Wavelet and Hierarchical Finite State Vector Quantization" *Proceedings of the 3rd International Symposium on Image and Signal Processing and Analysis2003 (ISPA2003)*, pp. 311-316, 2003.
- (Lu et al., 2000) J. Z. M. Lu, J. S. Pan and S. H. Sun, "Image Coding Based On Classified Side-Match Vector Quantization," *IEICE Transaction Information System*, E83-D, no. 12, December 2000.
- (Lu et al., 2002) Z. M. Lu, B. Yang and S. H. Sun, "Image Compression Algorithms Based On Side-Match Vector Quantization With Gradient-Based Classifiers," *IEICE Transaction Information System*, E85-D, no. 9, September 2002.
- (Nadenau et al., 2003) M. J. Nadenau, J. Reichel and M. Kunt, "Wavelet-Based Colour Image Compression: Exploiting the Contrast Sensitivity Function", *IEEE Transaction on Image Processing*, vol. 12, no. 1, pp. 58-70, January 2003.
- (Ostermann et al., 2004) J. Ostermann, J. Bormans, P. List, D. Marpe, M. Narroschke, F. Pereira, T. Stockhammer, and T. Wedi, "Video coding with H.264/AVC: Tools, Performance, and Complexity," *IEEE Circuits and System Magazine*, Vol. 4, No. 1, pp. 7-28, First Quarter 2004.

- (Peng & Kieffer, 2004) K. Peng and J. C. Kieffer, "Embedded Image Compression Based on Wavelet Pixel Classification and Sorting," *IEEE Transaction on Image Processing*, vol. 13, no. 8, pp. 1011-1017, August 2004.
- (Said & Pearlman, 1996) A. Said and W. Pearman, "A new, Fast, and Efficient Image Codec Based on Set Partitioning in Hierarchical Trees", *IEEE Transaction on Circuits and Systems for Video Technology*, Vol. 6, no. 3, pp. 243-250, June 1996.
- (Saryazdi & Jafari, 2002) S. Saryazdi and M. Jafari, "A High Performance Image Coding Using Uniform Morphological Sampling, Residues Classifying, and Vector Quantization," *EurAsia-ICT 2002*, Shiraz, Iran, October 2002.
- (Scargall & Dlay, 2000) L. D. Scargall and S. S. Dlay, "New methodology for adaptive vector quantization", *IEE Proceedings on Vision, Image and Signal Processing*, Vol. 147, No. 6, December 2000.
- (Shapiro, 1993) J.M Shapiro, "Embedded image coding using zerotrees of wavelet coefficients", *IEEE Transactions on Acoustics, Speech, and Signal Processing*, vol. 41, Issue 12, pp. 3445 - 3462, 1993.
- (Sheikh Akbari & Soraghan, 2003) A. Sheikh Akbari and J.J. Soraghan, "Adaptive Joint Subband Vector Quantization Codec For Handheld Videophone Applications", *International Journal of IEE Electronic Letters*, VOL. 39. NO.14, pp. 1044 - 1046, 2003.
- (Skodras et al, 2001) A. Skodras, Ch. Christopoulos, and T. Ebrahimi, "The JPEG 2000 Still Image Compression Standard," *IEEE Signal Processing Magazine*, vol. 18, no.5, September 2001.
- (Tan et al, 2004) D. M. Tan, H. R. Wu, and Z. Yu, "Perceptual Coding of Digital Monochrome Images," *IEEE Signal Processing Letters*, Vol. 11, no. 2, pp. 239-242, February 2004.
- (Thornton et al., 2002) L. Thornton, J. Soraghan, R. Kutil, M. Chakraborty, "Unequally protected SPIHT video codec for low bit rate transmission over highly error-prone mobile channels," *Elsevier Science: Signal Processing: Image Communication*, vol. 17, pp. 327-335, 2002.
- (Valade & Nicolas, 2004) C. Valade, J. M. Nicolas, "Homomorphic wavelet transform and new subband statistics models for SAR image compression" *IEEE International Proceedings on Geoscience and Remote Sensing Symposium, IGARSS 2004*, Vol.1, 2004.
- (Van Dyck & Rajala, 1994) R.E. Van Dyck, and S. A. Rajala, "Subband/VQ Coding of Colour Images with Perceptually Optimal Bit Allocation", *IEEE Trans. on Circuits and Systems for Video Technology*, vol. 4, no. 1, February 1994.
- (Voukelatos & Soraghan, 1997) S. P. Voukelatos and J. J. Soraghan, "Very Low Bit Rate Color Video Coding Using Adaptive Subband Vector Quantization with Dynamic Bit Allocation", *IEEE Transaction on Circuits and Systems for Video Technology*, vol. 7, no. 2, pp. 424-428, April 1997.
- (Voukelatos & Soraghan, 1998) S. P. Voukelatos and J. J. Soraghan, "A multiresolution adaptive VQ based still image codec with application to progressive image transmission", *EURASIP Signal Processing: Image Communication*, vol. 13, no. 2, pp. 135-143, 1998.
- (Wang et al., 2001) J. Wang, W. Zhang and S. YU, "Wavelet coding method using small block DCT," *Electronic Letters*, Vol. 37, No. 10, pp.627-629, May 2001.
- (Yovanof & Liu, 1996) Yovanof and S. Liu, "Statistical analysis of the DCT coefficients and their quantization error", *Thirtieth Asilomar Conference on Signals, Systems and Computers*, pp. 601-605, 1996.



Advances in Wavelet Theory and Their Applications in Engineering, Physics and Technology

Edited by Dr. Dumitru Baleanu

ISBN 978-953-51-0494-0

Hard cover, 634 pages

Publisher InTech

Published online 04, April, 2012

Published in print edition April, 2012

The use of the wavelet transform to analyze the behaviour of the complex systems from various fields started to be widely recognized and applied successfully during the last few decades. In this book some advances in wavelet theory and their applications in engineering, physics and technology are presented. The applications were carefully selected and grouped in five main sections - Signal Processing, Electrical Systems, Fault Diagnosis and Monitoring, Image Processing and Applications in Engineering. One of the key features of this book is that the wavelet concepts have been described from a point of view that is familiar to researchers from various branches of science and engineering. The content of the book is accessible to a large number of readers.

How to reference

In order to correctly reference this scholarly work, feel free to copy and paste the following:

Pooneh Bagheri Zadeh, Akbar Sheikh Akbari and Tom Buggy (2012). Wavelet Based Image Compression Techniques, *Advances in Wavelet Theory and Their Applications in Engineering, Physics and Technology*, Dr. Dumitru Baleanu (Ed.), ISBN: 978-953-51-0494-0, InTech, Available from:

<http://www.intechopen.com/books/advances-in-wavelet-theory-and-their-applications-in-engineering-physics-and-technology/wavelet-based-image-compression-techniques>

INTECH

open science | open minds

InTech Europe

University Campus STeP Ri
Slavka Krautzeka 83/A
51000 Rijeka, Croatia
Phone: +385 (51) 770 447
Fax: +385 (51) 686 166
www.intechopen.com

InTech China

Unit 405, Office Block, Hotel Equatorial Shanghai
No.65, Yan An Road (West), Shanghai, 200040, China
中国上海市延安西路65号上海国际贵都大饭店办公楼405单元
Phone: +86-21-62489820
Fax: +86-21-62489821

© 2012 The Author(s). Licensee IntechOpen. This is an open access article distributed under the terms of the [Creative Commons Attribution 3.0 License](#), which permits unrestricted use, distribution, and reproduction in any medium, provided the original work is properly cited.